



Hydroforming process of thin-walled tubular components with multiple local bulges

Xiao-Lei Cui¹ · Ju Guo^{2,3} · Yuanyang Zhao¹ · Peng Lin³

Received: 3 January 2023 / Revised: 6 May 2023 / Accepted: 4 June 2023 / Published online: 15 June 2023
© Wrocław University of Science and Technology 2023

Abstract

In the hydroforming process of a thin-walled tubular component with multiple local bulges, the bulge in the middle position is almost impossible to be formed with a conventional one-step hydroforming process because of the difficult axial feeding. To solve this problem, a novel method is proposed by preforming wrinkles using selective induction heating at different positions of tube blank to aggregate materials in advance for the subsequent hydroforming of tubular component with multiple local bulges. In this paper, the wrinkling behavior of 5052 aluminum alloy tube blank under different conditions and the deformation behavior of the wrinkled tube blank in subsequent hydroforming process of tubular component with three bulges are analyzed. It is shown that the existence of wrinkles is beneficial to increase the ultimate expansion ratio of the tube blank. Moreover, the instability behavior of multiple wrinkles on 5052 aluminum alloy tube blanks under different conditions was investigated by experiments. The process parameters for prefabricating two or three wrinkles, including temperature, spacing between wrinkles, and internal pressure, were determined through a detailed experimental investigation. Finally, the defects including splitting and undercut that occur in the hydroforming of tubular component with three bulges are analyzed, and the thin-walled tubular component with three bulges was hydroformed successfully using a wrinkled tube blank obtained under the process parameters of 250 °C, 4 mm, 5.5 MPa/350 °C, 10 mm, 2 MPa/400 °C, 6 mm, 1.33 MPa. These results provide insights for the manufacturing of tubular component with multiple local bulges from hard-to-form materials.

Keywords Hydroforming · Wrinkling behavior · Non-uniform temperature field · Induction heating · Tubular component with three bulges

1 Introduction

As an advanced lightweight manufacturing technology, hydroforming process can be used to form thin-walled tubular components with high expansion ratio, and can greatly reduce weight, improve stiffness and fatigue strength [1]. However, for the tube materials with low formability, such as aluminum alloy [2] and magnesium alloy [3] widely used in industrial field, problems such as uneven distribution of wall

thickness, splitting and wrinkling are easy to occur when the variable-diameter tubular component with large expansion ratio is manufactured using hydroforming technology [4]. In the hydroforming process of variable-diameter tubular components with local expansion bulges, axial feeding is very important, because the tube blank with low formability tends to split before it attaches on the die cavity under the action of internal pressure without insufficient axial feeding [5]. The higher number of local bulges, the greater the amount of axial feeding required. Especially, when the variable-diameter tubular component has three local bulges at different positions along the centerline, it is very difficult to form the bulge in the middle position. This is because the material is difficult to be fed to the middle position due to the existence of the bulges on both sides in conventional one-step hydroforming process. Even if the variable-diameter tubular component with multiple local bulges can be successfully obtained, the ultimate expansion ratio of bulge is also very low. This is because that the formability of tubes

✉ Xiao-Lei Cui
xiaoleicui@hit.edu.cn

¹ National Key Laboratory for Precision Hot Processing of Metals, Harbin Institute of Technology, Harbin 150001, China

² China National Heavy Duty Truck Group Datong Gear Co., Ltd., Datong 037000, China

³ College of Materials Science and Engineering, Taiyuan University of Technology, Taiyuan 030024, China

decreases as the number of expansion bulges along the centerline increases in hydroforming. If a component has more than three local bulges placed on different axial positions, it is almost certainly unfeasible [6].

To increase the ultimate expansion ratio of variable-diameter tubular components, a novel hydroforming process with useful wrinkled tube blank was proposed [7]. In this process, useful wrinkles are first preformed on the tube blank in the hydroforming die cavity by reasonable matching of axial feeding and internal pressure, and then the wrinkles are flattened and attached to the die cavity by increasing internal pressure to form a tubular component with large expansion ratio. Through finite element analysis, Lang et al. [8] found that obtaining appropriate shape of wrinkles by controlling internal pressure and axial feeding in preforming stage is very important for the flattening of wrinkles in the calibration stage, and an appropriate internal pressure can make the thickness distribution in the bulging area more uniform. They also found that a preforming die with 25° transition area is more likely to produce useful wrinkles than a 45° preforming die [9]. Tang et al. [10] studied the wrinkling and flattening behavior of AZ31B magnesium alloy tube blanks under different loading paths at high temperature, and analyzed the wrinkles characteristics and the effect of loading paths on ultimate expansion ratio. Song et al. [11] proposed a new numerical simulation method to design the preforming shape based on deformation history to improve the formability of the tube blank. The preforming shape is actually a useful wrinkle that can be flattened in the calibration stage, and a tubular component with uniform wall thickness can be obtained using this method. In addition, the wrinkling behavior of thin-walled tubes under double-sided pressures is systematically studied [12]. It was found that the contour shape of the wrinkle did not change with the external pressure when the pressure difference was constant. When the internal pressure was constant, increasing of the external pressure can suppress the formation of the middle wrinkle. At present, the above-mentioned method of preforming useful wrinkled tubes in die cavity has been successfully applied to the forming of variable-diameter tubular components with a single expansion bulge. During the hydroforming process, the multiple wrinkles formed in the preforming stage are flattened into a larger expansion bulge under the action of internal pressure. However, there are some difficulties in hydroforming tubular components with multiple local bulges using the above method. First of all, the formation and development of wrinkles depend heavily on the inclination angle of the transition area of the die cavity. Second, the number and relative position of wrinkles are difficult to control when multiple wrinkles would be preformed. In this case, it is not possible to accurately obtain the wrinkled tube blanks required for final tubular components with multiple local bulges.

In fact, the process of creating metal bellows is a process of preforming wrinkles on the tube blank. The conventional methods used to manufacture metal bellows mainly include joining smaller formed pieces, roll forming, mechanical bulging, and hydroforming [13]. However, the process of controlling the corrugation of bellows using above methods is complicated and affected by the die structure. In recent years, it has been found that local heating can be used to drive the development of wrinkles on tube blank combined with axial compression. Based on this principle, tubular component with multiple local wrinkles can be precisely prefabricated. Furushima et al. [14] proposed a semi-dieless metal bellows forming process, using which metal bellows with continuous wrinkles can be successfully produced. However, this method does not completely get rid of the influence of rigid die. A mandrel is installed inside the tube blank to ensure that the tube blank is subjected to uniform compressive force along the axial direction, and wrinkling outward in the heating area. On this basis, Zhang et al. [15] proposed a dieless forming process for metal bellows, in which the mandrel is no longer needed as a support for the wrinkling. It was shown that the shape of bellows can be controlled by adjusting the compression ratio. Sedighi and Shamsi [16] proposed a new method for fabricating metal bellows by local arc heating and axial compression. Because the arc heating has the characteristic of energy concentration, there is no need to design a special cooling device. It is worth noting that the research on prefabricating wrinkled tubes by local heating mainly focused on small-sized 304 stainless steel tubes, and the obtained wrinkles are the waveform of the final bellows, which do not require secondary forming. To sum up, there are few researches on dieless forming of useful wrinkled tubes for aluminum alloys and magnesium alloys using local heating. The wrinkled tubes were never put into the hydroforming die cavity for manufacturing a variable-diameter tubular component with multiple expansion bulges and large expansion ratio.

Therefore, a new method of producing variable-diameter tubular component with multiple bulges was proposed in this paper [17]. In this method, the tube blank was locally heated to prefabricate useful wrinkles, and then hydroforming was performed. In this way, the forming limit of the variable-diameter tubular component can be improved. In this paper, the experimental material is 5052 aluminum alloy tube blank, and multiple useful wrinkles were locally prefabricated on it by selective induction heating. The investigations were systematically conducted on the wrinkling behavior of the tube blank, the hydro-bulging behavior, the variation of shape and size of wrinkles during the hydroforming process, and the axial thickness distribution. Then the mechanics analysis of wrinkling process was carried out to reveal the wrinkling mechanism of the 5052 aluminum alloy tube in non-uniform temperature field. Finally, a variable-diameter

tubular component with multiple bulges and large expansion ratio was produced.

2 Forming principle of thin-walled tubular component with multiple local bulges

Figure 1 is the schematic diagram for prefabricating a tube blank with multiple local useful wrinkles by selective induction heating. First, the induction heating coil is adjusted to the target position of the tube blank to be wrinkled, and then high-pressure gas is slowly pressurized inside the tube blank. When the internal pressure of the tube blank reaches a target value, the coil starts to inductively heat the area of the tube blank to be wrinkled. In this case, a non-uniform temperature field with higher temperature in the middle and a gradual decrease to both sides is formed along the axial direction of the tube blank. Once the highest temperature in the wrinkling zone reaches the target value, the heating is stopped and the axial compression is carried out. Under the combined action of axial compression and internal pressure, instability occurs first in the high-temperature zone of the tube blank, and the first axisymmetric wrinkle was formed.

After the temperature of the tube is cooled to room temperature, the coil is adjusted to the second position of the tube blank to be wrinkled. When the highest temperature at this position reaches the target value, the tube is compressed axially again to form the second axisymmetric wrinkle. By analogy, a wrinkled tube with multiple wrinkles can be finally obtained.

The prefabricated tube blank with multiple wrinkles is then put into the hydroforming die cavity, and internal pressure is applied to the tube inside after the dies are closed. With the increase of internal pressure, the multiple wrinkles on the tube blank were gradually expanded and flattened, and finally encountered to the die cavity. For calibration, the internal pressure is further increased for making the tube fully attached to the die cavity. At this moment, a variable-diameter tubular component with multiple bulges is obtained. The hydroforming principle of thin-walled tubular component with multiple local bulges is shown in Fig. 2.

Fig. 1 Schematic diagram for prefabricating tube blank with useful wrinkles by selective induction heating

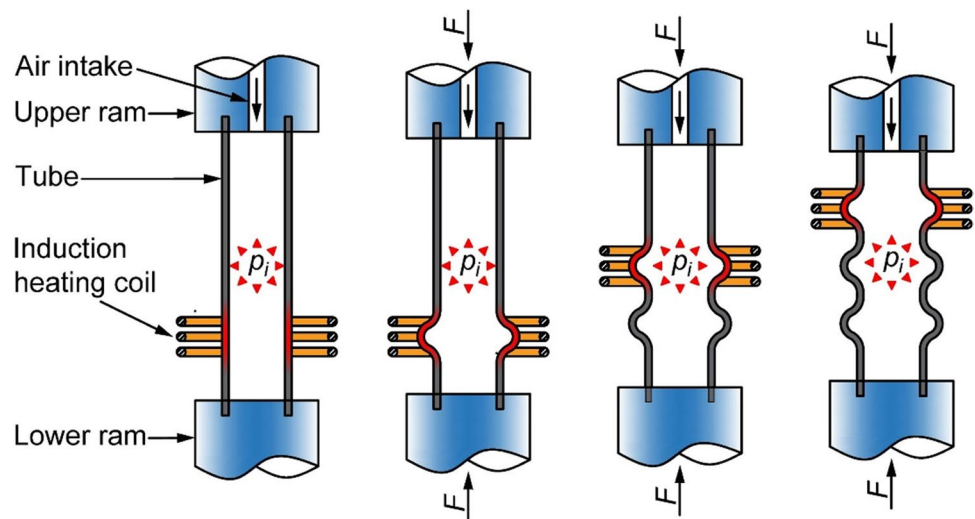


Fig. 2 Schematic diagram of hydroforming of thin-walled tubular component with multiple local bulges: **a** liquid filling; **b** calibration

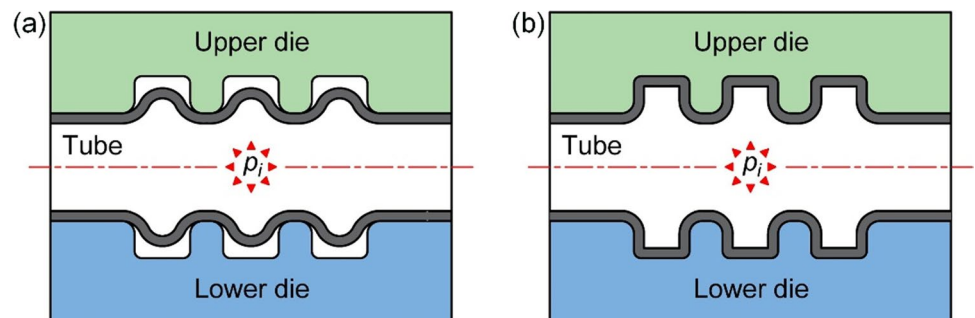


Fig. 3 Dimensions of the variable-diameter tubular component with three bulges

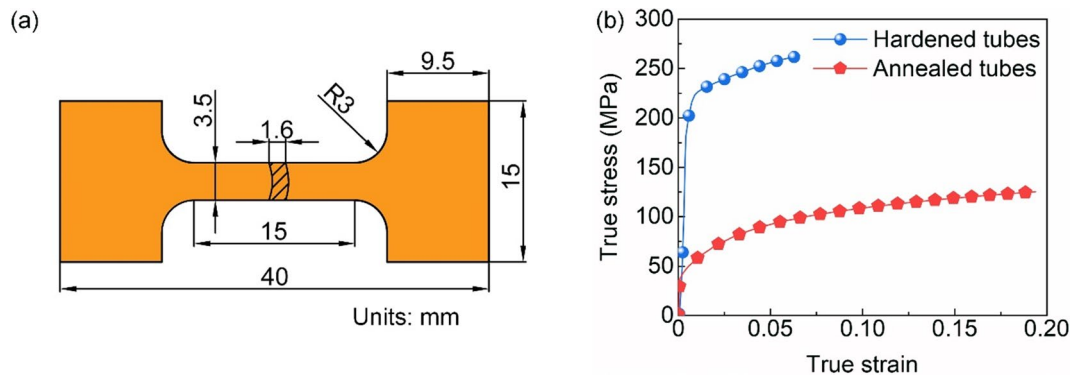
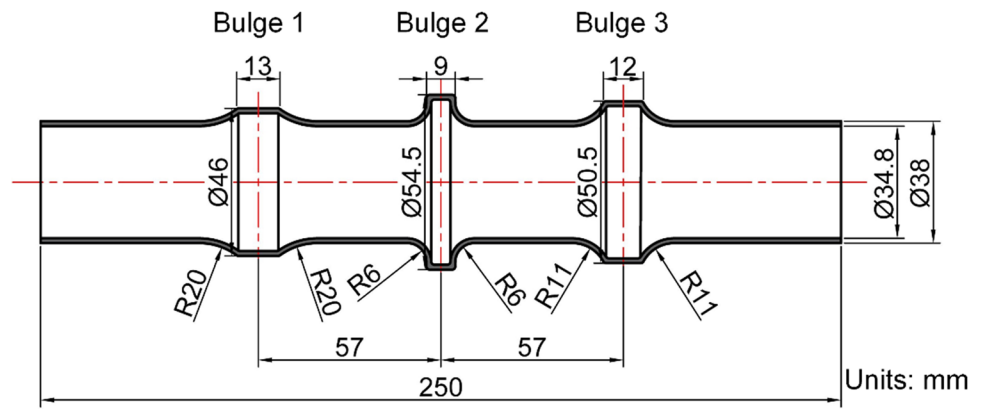


Fig. 4 Tensile test of 5052 aluminum alloy tube blank at room temperature: **a** dimensions of the specimen; **b** true stress–strain curve

3 Tubular component and methods

3.1 Geometric dimensions of tubular component with multiple bulges

Figure 3 shows the dimensions of the variable-diameter tubular component with three bulges to be formed. It can be seen from the figure that there are three bulges of different sizes at different positions along the axial direction of the tube. The diameters of bulges 1, 2, and 3 are Ø46 mm, Ø54.5 mm, and Ø50.5 mm, respectively. Obviously, the bulge 2 has the largest diameter and the smallest width, indicating the largest expansion ratio of the tube, while the diameters and widths of the bulges 1 and 3 are smaller. The expansion ratios of the three bulges from left to right relative to the initial straight tube blank are 21.1%, 43.4%, and 32.9%, respectively.

3.2 Tube material

The material used in the experiment is 5052 aluminum alloy tube blank with diameter of 38 mm and nominal

Table 1 Mechanical properties parameters of 5052 aluminum alloy tube blank at room temperature

Mechanical parameters	Hardened tubes	Annealed tubes
Ultimate tensile strength/MPa	242.6	101.8
Yield strength/MPa	194.8	55.4
Total elongation/%	12.8	33.8
Uniform elongation/%	6.5	19.4
Strength factor K /MPa	344.3	182.3
Strain hardening index n	0.099	0.226

wall thickness of 1.6 mm. There are two states of hardened and annealed tube blank, wherein the annealed tube blank was obtained by heating the hardened tube blank to 350 °C in the furnace for 2 h, and then cooling in the furnace. Figure 4(a) shows the dimensions of the tensile specimens, which were cut from the tube blanks along their axial direction. An UTM4304 electronic universal testing machine was used to carry out uniaxial tensile test at room temperature with a tensile rate of 0.1 s⁻¹ for three times. Figure 4(b) shows the true stress–strain curves of the 5052 aluminum alloy tube blank at room temperature, and the corresponding mechanical properties parameters

are given in Table 1. It can be found that the plasticity and formability of the 5052 aluminum alloy tube blank are relatively low at room temperature, especially the hardened tube blank.

3.3 Hydro-bulging test of wrinkled tube blank

Hydro-bulging test is needed to carry out to measure the formability of wrinkled tube blank. Figure 5 is the schematic diagram of hydro-bulging of wrinkled tube blank. First, the length of the bulging zone should be determined to adjust the positions of dies. Then the pressurized liquid is filled into the inside of the tube blank. As the internal pressure increases, the tube blank expands outward along the circumferential direction until it reaches the bulging limit and splits. In the hydro-bulging test, different stress states will be produced on the tube blank with different length-to-diameter ratios. The deformation of wrinkled tube blank under different length-to-diameter ratios of the bulging zone (L/d_0) can be realized by adjusting the distance between the die sets, which are 0.5:1, 0.75:1, 1.0:1, 1.5:1, 2.0:1, 2.5:1, 3.0:1. After the hydro-bulging experiments, the outer contour of the bulging zone of the tube is measured along the direction of the splitting. The ultimate expansion ratio of the wrinkled tube blank can be calculated according to the maximum diameter in the middle of the bulging zone.

The hydro-bulging tests were carried out on the initial straight tube blank and the wrinkled tube blank, respectively. When the initial straight tube blank was hydro-bulged, the length of the tube blank is 270 mm, and the length of the bulging zone is $0.5d$ (19 mm), $1d$ (38 mm), $2d$ (76 mm), and $3d$ (114 mm), respectively. When hydro-bulging was carried out on the wrinkled tube blank, the length of the bulging zone is $1d$. The wrinkled tube blanks were obtained under axial compression with 6 mm displacement and 1 mm/s speed at temperature of 250 °C. During axial compression process, different internal supporting pressures of 0 MPa, 2.7 MPa, 5.5 MPa, and 8.2 MPa were, respectively, used.

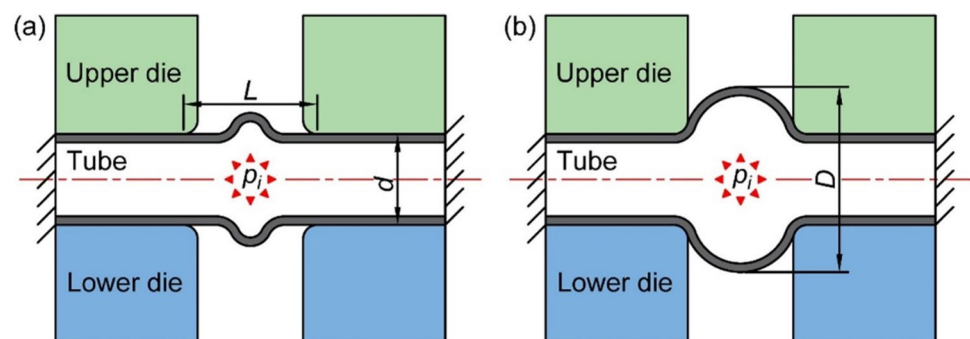
3.4 Experimental setup

3.4.1 Experimental setup for prefabricating wrinkled tube blanks

Figure 6 shows the experimental setup for prefabricating the wrinkled tube blanks by selective induction heating. As shown in the figure, the experimental setup mainly includes four parts: an axial compression unit, an induction heating unit, a booster unit, and a measuring/recording unit.

In the axial compression unit, the electronic universal testing machine is used to axially compress the tube blank. The PC can be used to set parameters, such as compression speed and compression displacement, and record the force–displacement curve in real time during the wrinkling process of the tube blank. The cooperation of the upper ram, the lower ram, the fixed rings, and the O-ring can realize the fixing and sealing for the tube ends. In the induction heating unit, the coil generates an alternating magnetic field to heat the tube blank and the heating speed is controlled by the induction heating device. Both ends of the coil are connected with cooling water pipes, to prevent the coil from being burned due to high temperature during the heating process. A water flow meter is connected to the inlet of the cooling water pipe, which is used to monitor the water flow in real time and to protect against water cutoff. In the booster unit, a N_2 cylinder provides high-pressure gas to the inside of the tube blank. The pressure reducing valve is used to adjust the output pressure of the N_2 cylinder. During the induction heating process, the safety valve is used to maintain the internal pressure of the tube blank within a certain range and plays a role of safety protection. The pressure gauge is used to monitor the internal pressure of the tube blank in real time, and its accuracy is within $\pm 0.5\%$. The measuring/recording unit, including a paperless recorder and a thermocouple, is used to measure the temperature of the heating area in real time.

Fig. 5 Schematic diagram of hydro-bulging of wrinkled tube blank: **a** liquid filling; **b** hydro-bulging



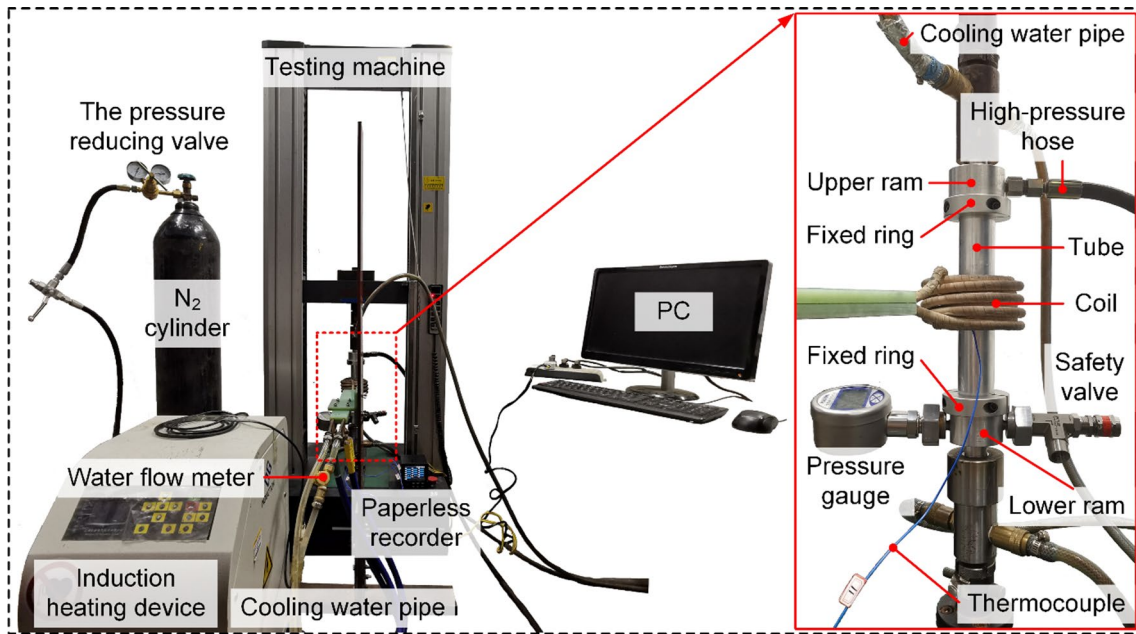


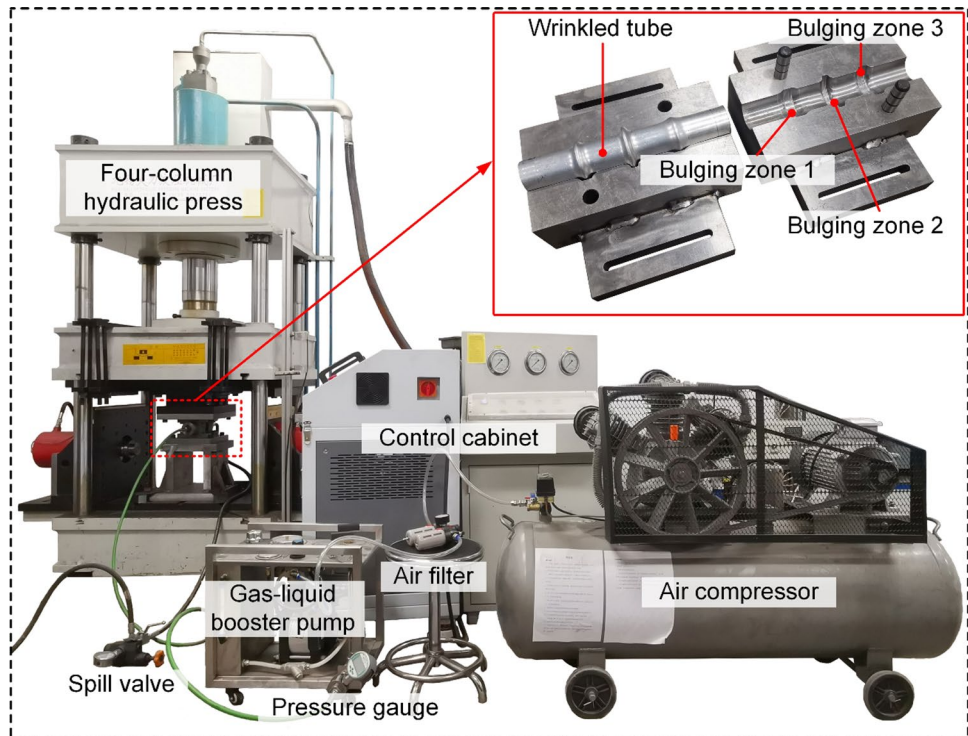
Fig. 6 Experimental setup for prefabricating wrinkled tube blanks by selective induction heating

3.4.2 Hydroforming experimental setup

Figure 7 shows the hydroforming experimental setup, which can be used for hydro-bulging and hydroforming experiments. As shown in the figure, it is built on a Y32-100 multifunctional four-column hydraulic press as the main body,

and the hydroforming dies required for different experiments can be clamped on its working platform. The closing and parting of the dies are realized by the hydraulic press. The high-pressure liquid required for the experiment can be provided by a gas-liquid booster pump, which can control the liquid pressure of emulsion to realize the functions of

Fig. 7 Hydroforming experimental setup



pressurizing, depressurizing, and maintaining the pressure inside the tube. The digital display pressure gauge is used to detect the output liquid pressure of the gas–liquid booster pump in real time. The spill valve can be used to exhaust all the air from the tube inside. At the same time, it can stabilize the internal pressure of tube blank and protect the safety of the whole system.

Based on the shape and size of the variable-diameter tubular component shown in Fig. 3, the hydroforming die was designed with three corresponding cavities (bulging zones). The distance between two adjacent cavities is 57 mm ($1.5d$). For ease of expression, the cavities on the die corresponding to bulges 1, 2, and 3 in Fig. 3 are marked as bulging zones 1, 2, and 3, respectively.

3.5 Experimental scheme

3.5.1 Experimental scheme for wrinkling

The influence of process parameters on the local instability behavior of the tube blank was investigated in this paper using the experiment when the second or more wrinkles will be preformed. The effect of process parameters, such as wrinkling temperature, spacing between wrinkles, and internal pressure, on the wrinkling behavior of multiple wrinkles of 5052 aluminum alloy tube blank was explored. The specific experimental scheme is shown in Tables 2 and

3, where p_s is the initial yield pressure of the tube blank, and d is the outer diameter of the tube blank.

In the experiment, the fixed length at both ends of the tube blank was 18 mm, respectively. The inner diameter of the heating coil was 56 mm, while the length of the heating zone was 36.6 mm. Moreover, the cooling water flow rate inside the coil was 4.96–5.27 L/min. In the wrinkling experiments of tube blanks with one and two wrinkles, the induction heating current was set as 27 A. In addition, in the wrinkling experiment of tube blank with three wrinkles, the induction current was set as 32 A to improve heating efficiency. During the axial compression process, the compression speed applied to the tube blank was 1 mm/s.

3.5.2 Experimental scheme for hydroforming

To produce the variable-diameter tubular component with three bulges shown in Fig. 3, a tube blank with three wrinkles must be prefabricated in sequence by induction heating. In the wrinkling experiment, the initial 5052 aluminum alloy tube blank was in a hardened state. The length of the used tube blank was 270 mm, the axial compression speed was 1 mm/s, and the induction heating current was 32 A. Hydroforming experiments would be carried out on the original straight tube blank and the prefabricated tube blank with three wrinkles, respectively. During the hydroforming process, the final calibration pressure was set as 54.25 MPa

Table 2 Experimental scheme for wrinkling of tube blank with two wrinkles

Tube state	Factor	Length/mm	Spacing/ d	Wrinkle 1			Wrinkle 2		
				Com- pression/ mm	Temperature/ $^{\circ}$ C	Internal pres- sure/MPa	Com- pression /mm	Temperature/ $^{\circ}$ C	Internal pressure/ MPa
Hardened	Temperature	188	$2d$	6	250	0	6	250, 275, 300, 325, 350	0
	Internal pres- sure	188	$1d$	6	250	5.5 ($0.4 p_s$)	6	250, 350	5.5 ($0.4 p_s$), 2 ($0.4 p_s$)
	Spacing	188	$0.5d, 1d,$ $1.5d, 2d$	6	250	0	6	250, 350, 400, 450	0
Annealed	Mechanical properties	188	$1d, 2d$	6	350	0	6	300, 350, 400	0

Table 3 Experimental scheme for wrinkling of tube blank with three wrinkles

Tube state	Length /mm	Spacing / d	Wrinkle 1			Wrinkle 2			Wrinkle 3		
			Com- pression / mm	Tem- perature / $^{\circ}$ C	Internal pressure / MPa	Com- pression / mm	Tem- perature / $^{\circ}$ C	Internal pressure / MPa	Com- pression / mm	Tem- perature / $^{\circ}$ C	Internal pressure / MPa
Hardened	188	1	6	250	0	6	350	0	6	450	0
	218	1.5	6	250	0	6	350	0	6	450	0

(3.5 ps). The flattening process of wrinkles and the defects that occurred in hydroforming was investigated to obtain the suitable wrinkling parameters. Finally, the thickness distribution of the variable-diameter tubular component with three bulges was analyzed.

4 Results and discussion

4.1 Hydro-bulging behavior of wrinkled tube blanks

Figure 8 shows the cracked tube specimens after hydro-bulging of the initial straight tube blanks under the condition of different length-to-diameter ratios and the wrinkled tube blanks obtained under different internal pressures. It can be seen from Fig. 8 that both kinds of tube blanks split along the axial direction in the bulging zone. However, the splitting position of the original tube blank is in the middle of the bulging zone, while that of the wrinkled tube blank is on one side of the wrinkle. According to previous research, it has been found that the thickening is the most serious at the wrinkle peak, followed by the wrinkle valley, and the least on the side of the wrinkle [18]. Therefore, the wall thickness on the side of the wrinkle is the thinnest in the wrinkled area. In addition, the heating and cooling during the wrinkling process for the wrinkle are equivalent to annealing treatment, which reduces the yield strength at this place. Therefore, in the hydro-bulging process, the splitting defect first occurs on the side of the wrinkle. Moreover, the

curvature radius at the side of wrinkle is larger than that at the peak and valley of wrinkle. It can be predicted that the side of wrinkle is subjected to greater tensile stress based on the stress equilibrium equation [19]. In this case, deformation and splitting are more likely to occur on the side of wrinkle under the same internal pressure.

Figure 9(a) shows the axial geometric contours of the cracked tube specimens after hydro-bulging of the initial straight tube blanks under different lengths of bulging zone. It can be seen from the figure that the tube blanks expand uniformly outward at the bulging zone until they split. Figure 9(b) shows the axial contour shapes of the cracked tube specimens from the wrinkled tube blanks under different support internal pressures. It can be seen from the figure that expansion deformation first occurs on the side of the wrinkle with the increase of the internal pressure during the hydro-bulging test. Then the deformation range gradually expands toward the wrinkle peak. When the internal pressure for wrinkling is 5.5 MPa or above, expansion deformation occurs in the whole bulging zone during hydro-bulging process.

Figure 10(a) shows the ultimate expansion ratio of the initial straight tube blanks under different lengths of the bulging zone. It is shown that the ultimate expansion ratio of the hardened tube blank decreases from 8.26% to 3.37% when the length of the bulging zone increases from $0.5d$ to $3d$. Figure 10(b) shows the ultimate expansion ratio of the wrinkled tube blanks obtained under different internal pressures. It can be found that the ultimate expansion ratios of the wrinkled tube blanks are 25.39%, 28.37%, 25.97%, and

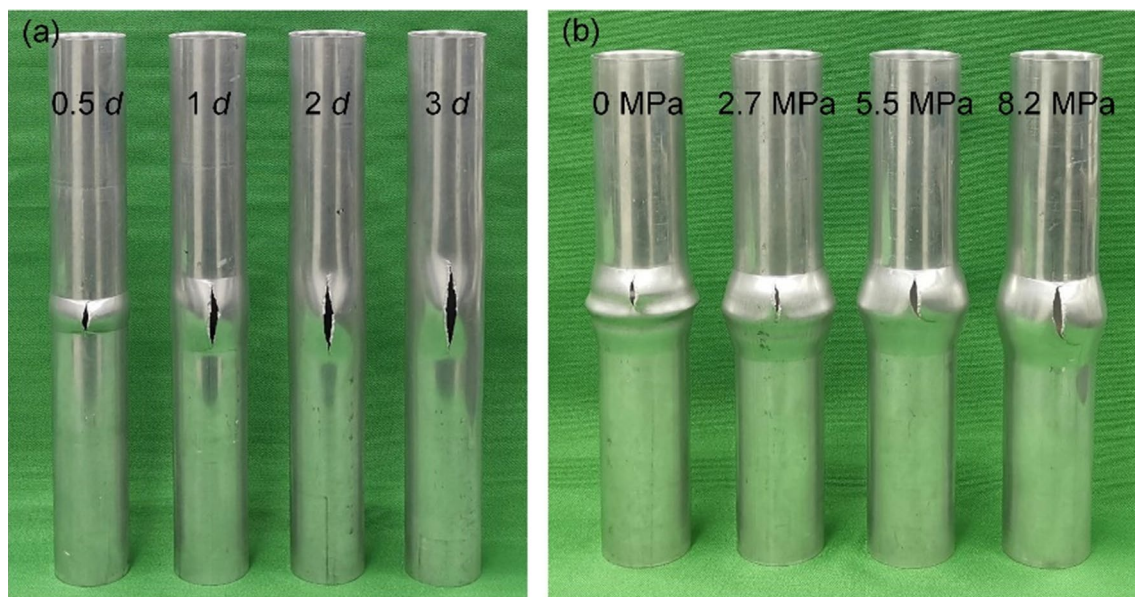


Fig. 8 Cracked tube specimens after hydro-bulging tests: **a** initial straight tube blanks; **b** wrinkled tube blanks obtained under different internal pressures

Fig. 9 Axial geometric contour of the cracked tube specimens: **a** initial straight tube blanks; **b** wrinkled tube blanks obtained under different internal pressures

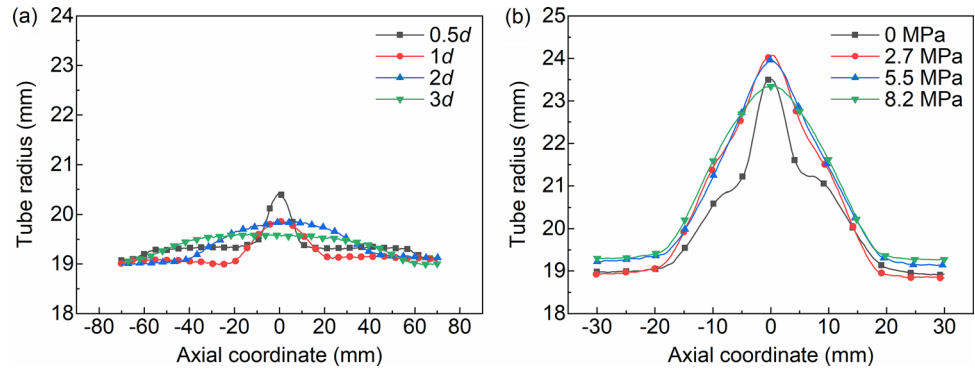
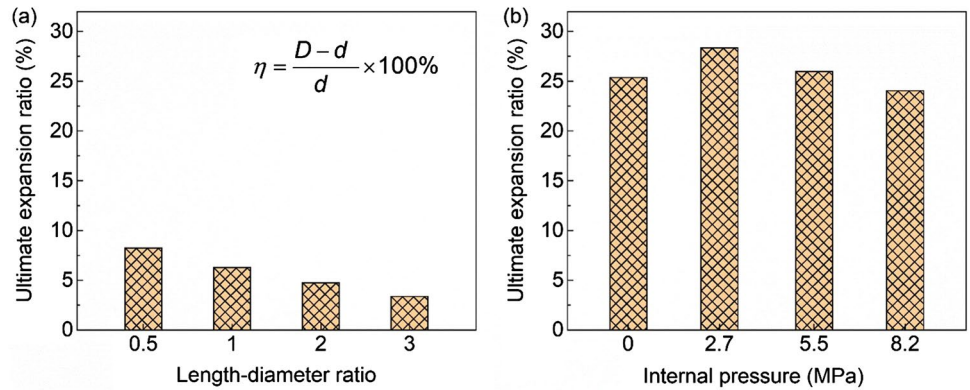


Fig. 10 Ultimate expansion ratio: **a** initial straight tube blanks; **b** wrinkled tube blanks



24.05%, respectively, with a maximum difference of 4.32%. This indicates that the existence of wrinkles is beneficial to increase the ultimate expansion ratio of the tube blank.

4.2 Wrinkling behavior of tube blank under different conditions

4.2.1 Wrinkling behavior of two wrinkles under different temperatures

Figure 11 shows the wrinkled tube specimens obtained by prefabricating the second wrinkle on the tube blank at different temperatures (indicated by the highest temperature in the heating zone). The first wrinkles were all prefabricated at 250 °C. In the figure, only the first wrinkle was prefabricated on the first tube blank on the left for comparison with the tube blank with two wrinkles. It is shown that wrinkling trend appears at the second wrinkling position to form tiny wrinkles when the temperature is 300 °C. When the temperatures are 325 °C and 350 °C, axisymmetric wrinkles are formed at the second wrinkling position. This indicates that the temperature for wrinkling at the second position needs to be higher than 300 °C after the first wrinkle is formed at 250 °C. In this case, a high enough temperature gradient can be produced along the axial direction of the tube blank to form an axisymmetric wrinkle.

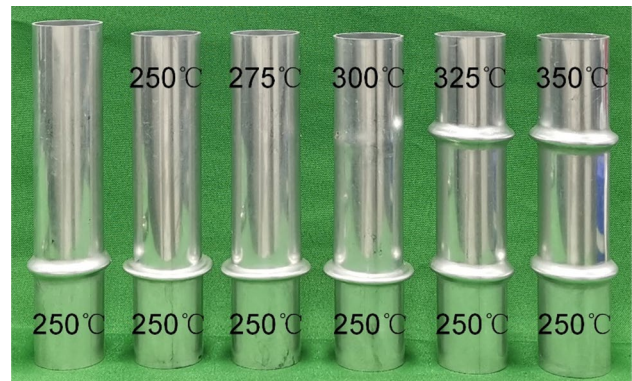


Fig. 11 Double wrinkled tube specimens obtained by prefabricating the second wrinkle at different temperatures

Figure 12 gives the force–displacement curves during the prefabricating process of wrinkled tube blanks with two wrinkles at different temperatures. In the force–displacement curves, the difference between the maximum force for forming the second wrinkle and the force at the end of forming the first wrinkle is defined as $\Delta F'$. It can be found that $\Delta F'$ decreases from 1.69 to -5.31 KN with the increase of wrinkling temperature for forming the second wrinkle from 250 to 350°C. This indicates that the higher the temperature for forming the second wrinkle, the lower the value of $\Delta F'$, the

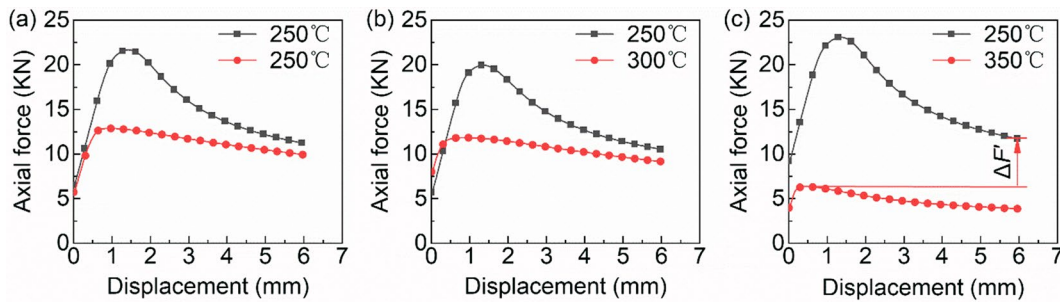


Fig. 12 Force–displacement curves during the prefabricating process of the two wrinkles at different temperatures: **a** 250 °C; **b** 300 °C; **c** 350 °C

more likely it is to form the second wrinkle. According to current experimental results, the second wrinkle is likely to be formed when the $\Delta F'$ is negative. In other words, the axial force required for the formation of the second wrinkle does not lead to further destabilization of the first wrinkle. However, since the temperature field at the first wrinkle has changed during the fabrication of the second wrinkle, the discussion on the formation condition of the second wrinkle based on force–displacement curve is only qualitative, which needs to be explored in further investigation.

Figure 13(a) shows the axial contour shape of the wrinkled tube blanks obtained under different temperatures of 250 °C, 300 °C, and 350 °C for the second wrinkle. It was found that the height and width of the first wrinkle formed at 250 °C were 3.89 mm and 2.47 mm, respectively. When the second wrinkle is prefabricated at 250 °C and 300 °C, it not only fails to form the second wrinkle, but also causes the first wrinkle to continue to destabilize, increasing in height and decreasing in width. When the second wrinkle

is prefabricated at 350 °C, the height of the two wrinkles is 4.45 mm and 4.87 mm, and the width is 2.33 mm and 2.37 mm. It can be found that formation of the second wrinkle at temperature of 350 °C has less effect on the size of the first wrinkle. Moreover, the shape and size of the second wrinkle are basically the same as that of the first wrinkle, and their shape can be accurately described by GaussAmp function with a fitting degree higher than 0.994.

Figure 13(b) shows the thickness distribution of the wrinkled tube blanks when the second wrinkle was produced at temperature of 350 °C. It can be found that the first wrinkle and the second wrinkle have the same distribution of thickness. The thickness of the tube blank in the wrinkled area is all increased under the axial compression. The slightest thickening is at the side of the wrinkle, and the thickening increases gradually toward the wrinkle peak and the wrinkle valley. Moreover, the wall thickness at the wrinkle peak is higher than that at the wrinkle valley.

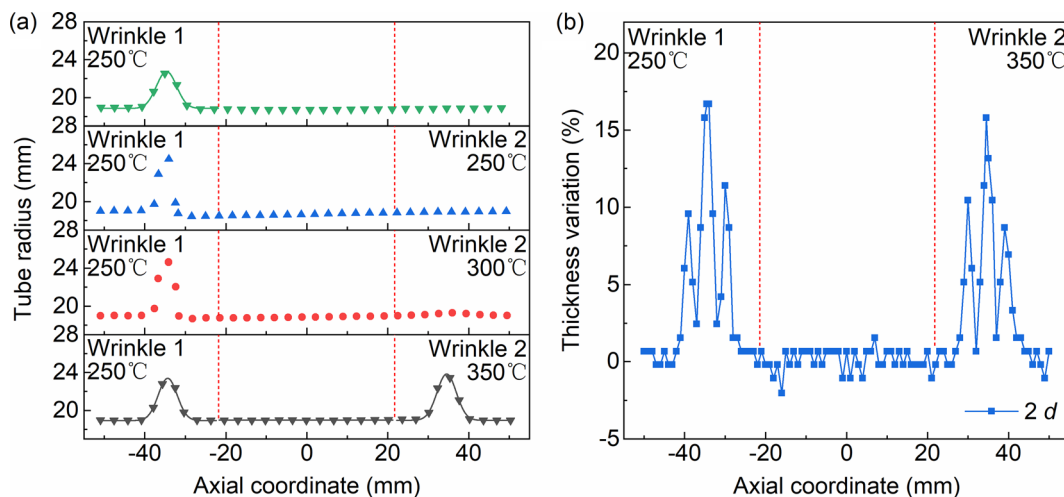


Fig. 13 Axial contour shape and thickness distribution of the wrinkled tube blanks obtained under different temperatures: **a** contour shape; **b** thickness distribution

4.2.2 Wrinkling behavior of two wrinkles with different spacings

Figure 14 shows the wrinkled tube specimens with two wrinkles having different spacings. It is shown that the second axisymmetric wrinkles can be formed on the tube blank at the temperature of 350 °C when the spacing is $2d$, $1.5d$, and $1d$, and it has little effect on the first wrinkles that have already formed. When the spacing is $0.5d$, the second wrinkle cannot be formed because the existing induction coil cannot be used to form a wide enough temperature gradient field along the axial direction of the tube blank.

Figure 15(a) shows the axial contour shape of the wrinkled tube blanks with two wrinkles having different spacing of $2d$, $1.5d$, and $1d$. As shown in the figure, the shape of

double wrinkles with different spacing can be accurately fitted by GaussAmp function, and the fitting degree is higher than 0.993. Moreover, it is shown that the width of the second wrinkle is 2.369 mm, 2.363 mm, and 2.388 mm, while its height is 4.866 mm, 4.642 mm, and 4.766 mm, when the spacing is reduced from 2 to $1d$. The maximum difference in the width and height of the second wrinkle is only 0.025 mm and 0.224 mm, which indicates that it has little influence on the formation of the second wrinkle when the spacing is greater than $1d$. Figure 15(b) shows the thickness distribution of the wrinkled tube blanks with two wrinkles. It can be seen from the figure that the thickness distributions of the tube blank at the two wrinkles are basically the same, and the spacing has very little effect on the thickness distribution of the two wrinkles.

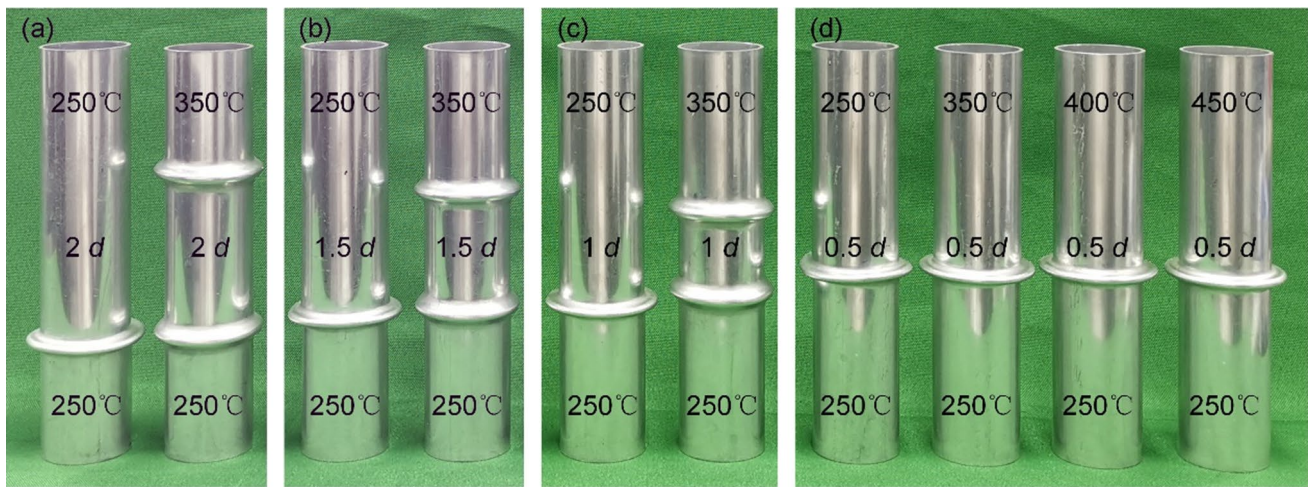


Fig. 14 Wrinkled tube specimens with two wrinkles having different spacing: **a** $2d$; **b** $1.5d$; **c** $1d$; **d** $0.5d$

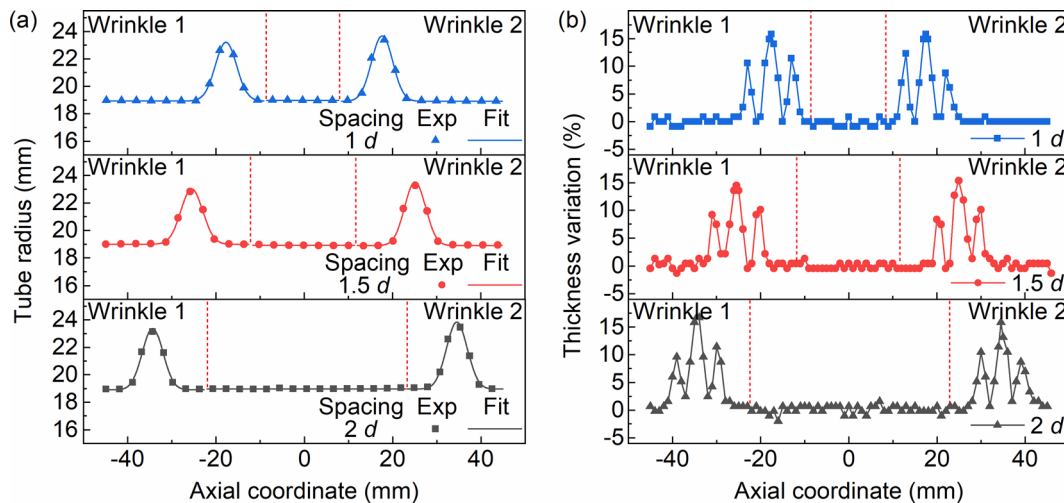


Fig. 15 Axial contour shape and thickness distribution of the wrinkled tube blanks with two wrinkles having different spacing: **a** contour shape; **b** thickness distribution

4.2.3 Wrinkling behavior of two wrinkles under different internal pressures

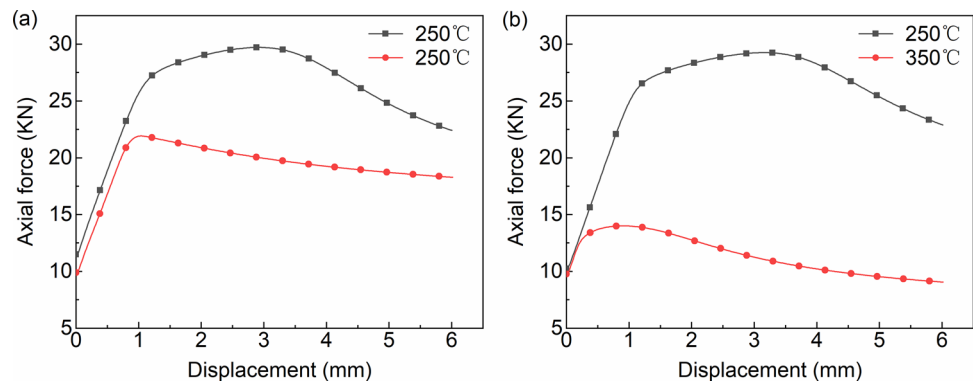
Figure 16 shows the wrinkled tube specimens with two wrinkles obtained under different internal pressures. The first wrinkle on the tube blanks was prefabricated under an internal pressure of 5.5 MPa at the temperature of 250 °C. If the same process conditions are used to prefabricate the second wrinkle, the first wrinkle will continue to undergo compression instability, and the second wrinkle cannot be formed. It is shown that the second axisymmetric wrinkle can be obtained successfully when the temperature for wrinkling is raised to 350 °C even if the internal pressure is only 2 MPa. In this case, the first wrinkle is unaffected.

Figure 17 shows the force–displacement curves during the prefabricating process of two wrinkles under different internal pressures and temperatures for the second wrinkle. It is shown that the second wrinkles cannot be formed



Fig. 16 Wrinkled tube specimens with two wrinkles obtained under different internal pressures

Fig. 17 Force–displacement curves during the prefabricating process of two wrinkles under different internal pressures and temperatures for the second wrinkle: **a** 5.5 MPa, 250 °C; **b** 2 MPa, 350 °C



on the blank under the conditions of internal pressure of 5.5 MPa and temperature of 250 °C, because $\Delta F'$ is basically close to zero (-0.49 KN) at this time. If the temperature is raised to 350 °C and the internal pressure is 2 MPa, $\Delta F'$ can be reduced to -8.89 KN, and the second wrinkle can be formed. In addition, compared with the wrinkling process without internal pressure, the internal pressure could make the maximum axial compressive force greater required for the formation of the second wrinkle greater.

Figure 18(a) shows the axial contour shape of the wrinkled tube blanks with two wrinkles obtained under internal pressure supporting. It is shown that the shape of the two wrinkles could be accurately fitted by GaussAmp function, and the fitting degree was 0.999, indicating a high fitting degree. The width of the two wrinkles is 4.863 mm and 3.247 mm, and the height is 4.039 mm and 5.177 mm, respectively. Compared with the wrinkling process of two wrinkles spaced $1d$ apart without internal pressure, it can be found that the existence of internal pressure makes the width of both wrinkles to increase.

Figure 18(b) shows the thickness distribution of the wrinkled tube blank with two wrinkles obtained under internal pressure supporting. It was found that thickening and thinning occur on the two wrinkles at the same time. The thickness variation of the whole tube blank is within the range of -2.56% to 6.04% , and the distribution of the wall thickness is relatively uniform.

4.2.4 Wrinkling behavior of two wrinkles for different tube materials

Figure 19 shows the wrinkling behavior of the annealed tube blank for prefabricating two wrinkles having different spacings. Compared with the hardened tube blank, the first wrinkle can be formed on the annealed tube blank at a higher temperature of 350 °C. When the second wrinkle was prefabricated (the wrinkle spacing was $2d$), there was only a tendency to wrinkle at 350 °C. When the temperature for wrinkling reaches 400 °C, the second wrinkle can be formed successfully. This indicates that the second wrinkle can be

Fig. 18 Axial contour shape and thickness distribution of the wrinkled tube blanks with two wrinkles obtained under internal pressure supporting: **a** contour shape; **b** thickness distribution

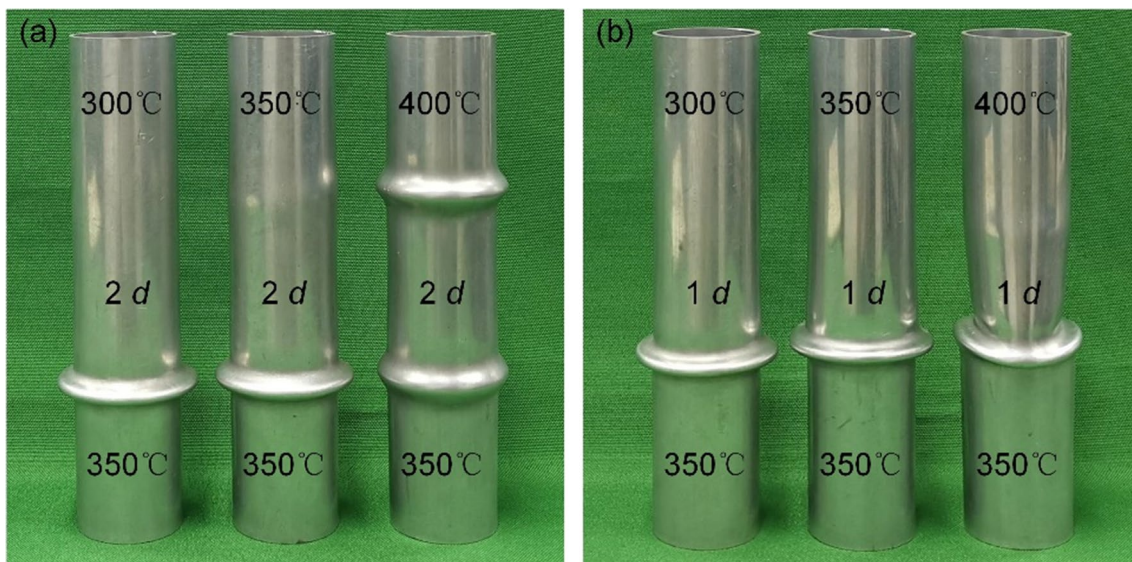
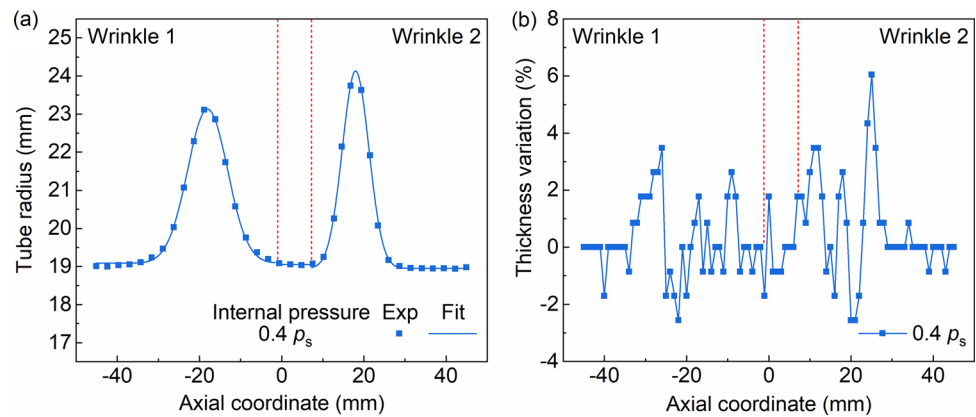


Fig. 19 Wrinkling behavior of the annealed tube blank for prefabricating two wrinkles having different spacings: **a** $2d$; **b** $1d$

formed on the annealed tube blank under a lower temperature difference on the basis of the first wrinkle. However, the temperature for wrinkling of the annealed tube blank is higher than that of the hardened tube blank. Moreover, if induction heating is conducted $1d$ away from the first wrinkle, the second wrinkle cannot be formed at temperatures from 300°C to 400°C , and will cause the first wrinkle to distort.

Figure 20 shows the force–displacement curves during the prefabricating process of the two wrinkles with a distance of $2d$ for the annealed tube blanks under different temperatures. It is shown that $\Delta F'$ is 1.6 KN, 0.81 KN, and 0.31 KN, respectively, when the wrinkling temperature for prefabricating the second wrinkle increases from 300°C to 350°C , and then to 400°C . The value of $\Delta F'$ close to 0 at 400°C makes it easier to form the second wrinkle, which is consistent with the wrinkling behavior of hardened tube blank.

Figure 21(a) shows the axial contour shape of the two wrinkles with a spacing of $2d$ for the annealed tube blank. It is shown that the shape of the two wrinkles could be accurately fitted by GaussAmp function, and the fitting degrees are above 0.994. By analyzing the fitting function, it can be obtained that the width of the first wrinkle and the second wrinkle is 3.186 mm and 3.048 mm, and the height is 3.728 mm and 4.166 mm, respectively. Compared to the first wrinkle, the second wrinkle is smaller in width and larger in height because it is formed at higher temperature.

Figure 21(b) shows the thickness distribution of the annealed wrinkled tube blank with two wrinkles. It is shown that the thickness distribution of the first wrinkle and the second wrinkle is consistent. As with the hardened tube blank, the whole tube blank in the wrinkled area is thickened. The difference is that the wall thickness at the wrinkle valley of annealed tube blank is basically the same as that at the wrinkle peak, or thickening is more serious.

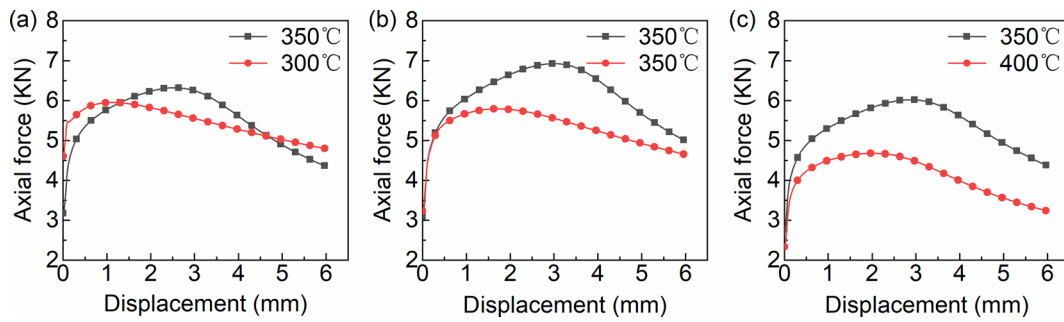
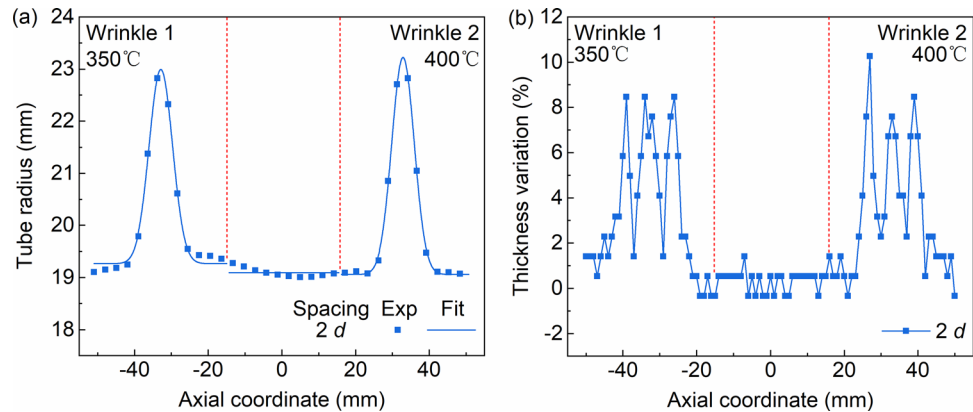


Fig. 20 Force–displacement curves during the prefabricating process of two wrinkles with a distance of $2d$ for the annealed tube blanks under different temperatures: **a** 300 °C; **b** 350 °C; **c** 400 °C

Fig. 21 Axial contour shape and thickness distribution of two wrinkles with a distance of $2d$ for the annealed tube blank: **a** contour shape; **b** thickness distribution



Besides, the thickness variations of the annealed tube blank at the first wrinkle and the second wrinkle are in the range of $-0.3\% \sim 8.5\%$ and $-0.3\% \sim 10.3\%$, while those of the hardened tube blank are in the range of $-0.2\% \sim 16.7\%$ and $-0.2\% \sim 15.8\%$, respectively. Obviously, the thickness variations of the annealed tube blank at the two wrinkles are smaller than that of the hardened tube blank.

4.2.5 Wrinkling behavior of three wrinkles

To verify the feasibility of forming multiple wrinkles by selective heating, wrinkling was carried out on three different positions of the tube blank in sequence. Figure 22(a) shows the wrinkled tube specimens for forming three wrinkles with different spacing. It is found that the third wrinkle cannot be formed when the spacing between wrinkles is $1d$. When the spacing increases to $1.5d$, axisymmetric wrinkles can be formed at three different positions due to the formation of a wide gradient temperature field along the axial direction of the tube blank. In addition, the formation of the third wrinkle does not affect the shape of the first and second wrinkles. Figure 22(b) is the axial contour shape of the three wrinkles with the spacing of $1.5d$. Similarly, the shape of the three wrinkles can be accurately described by GaussAmp function with a fitting degree higher than 0.99.

4.3 Hydroforming behavior of variable-diameter tubular component with three bulges

In the hydroforming process, the wrinkled tube blank with three wrinkles prefabricated by induction heating was used to produce a variable-diameter tubular component with three bulges. Therefore, to manufacture the variable-diameter tubular component with three bulges shown in Fig. 3, it is necessary to determine the appropriate process parameters to successfully prefabricate a wrinkled tube blank with three wrinkles. Otherwise, it is easy to produce some defects such as splitting in the hydroforming process. As can be seen from Fig. 3, the distance between adjacent bulges of the final hydroformed component is 57 mm. Therefore, according to the wrinkling results discussed in Sect. 4.2, the distance between adjacent positions on the initial tube blank for wrinkling is tentatively set as 67 mm. When the tube blank with three wrinkles is prefabricated, the wrinkling process parameters are represented by the marking method as shown in Fig. 23. At this moment, wrinkles 1, 2, and 3 on the wrinkled tube blank should have a correspondence to the bulging zones 1, 2, and 3 on the hydroforming die in Fig. 7 and the bulges 1, 2, and 3 of the tubular components in Fig. 3, respectively.

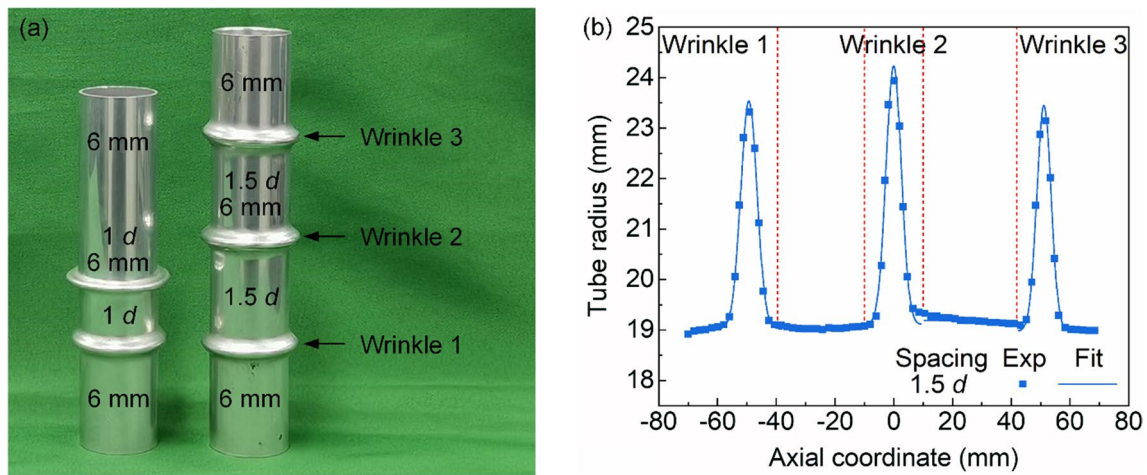


Fig. 22 Wrinkled tube specimen with three wrinkles and its axial contour shape: **a** tube specimens; **b** contour shape

Temperature, Compression, Internal gas pressure	/	Temperature, Compression, Internal gas pressure	/	Temperature, Compression, Internal gas pressure
Wrinkle 1		Wrinkle 2		Wrinkle 3

Fig. 23 Wrinkling process parameters representation for prefabricating wrinkled tube blank with three wrinkles

4.3.1 Defect analysis in hydroforming

Figure 24 shows the common defects occur in the hydroforming of the tubular component with three bulges. It can be found that the main defects are splitting and undercut. If the initial straight tube blank is directly used for hydroforming, due to the low plasticity of the tube blank, splitting occurred on the tube blank along the axial direction at the first bulge position when the internal pressure was loaded to 24.5 MPa, as shown in Fig. 24(a). At this time, the expansion ratios of the tube blank at the first, second, and third bulge positions are 4.53%, 3.32%, and 3.47%, respectively, and the expansion ratios are all small. Even if the axial feeding is applied, the material is difficult to be fed to the middle position due to the existence of the bulges on both sides in conventional one-step hydroforming process. This indicates that it is difficult to obtain the variable-diameter tubular component with three bulges through directly hydroforming of the initial straight tube blank.

When the wrinkled tube blank is used for hydroforming, splitting and undercut defects can also occur if the wrinkle size is not properly controlled, as shown in Fig. 24(b) and (c). For the wrinkled tube blank prefabricated under the process parameters of 250 °C, 6 mm, 0 MPa/350 °C, 6 mm, 0 MPa /400 °C, 6 mm, 0 MPa, the splitting occurs at the position of the second bulge along the circumferential direction when the internal pressure reaches 44.6 MPa in

subsequent hydroforming process, as shown in Fig. 24(b). This is mainly because the size of the prefabricated wrinkles is small, which is not enough to make up for the material required for the tube blank to be expanded to attach the die cavity. In addition, the wrinkle has not been completely flattened at the position of the first bulge because the internal pressure has not been loaded to the target value.

If the process parameters for wrinkling process are adjusted to 250 °C, 6 mm, 5.5 MPa/350 °C, 8 mm, 2 MPa /400 °C, 8 mm, 1.33 MPa, the undercut defect as shown in Fig. 24(c) is produced in the subsequent hydroforming process at the positions of the first and third bulges. This is because the size of the first and third prefabricated wrinkles is too large to be completely put into the corresponding position of the die cavity, and the defect of undercut occurs during the die closing process. However, at the position of the second bulge, the tube blank did not fully stick to the die cavity due to the smaller size of wrinkle.

4.3.2 Hydroforming process of wrinkled tube blanks

To avoid splitting and undercut defects in subsequent hydroforming process, the axial compression for prefabricating the first and third wrinkles is reduced to 4 mm and 6 mm respectively, while it is increased to 10 mm for prefabricating the second wrinkle during the wrinkling process. In this case, the process parameters of wrinkling for prefabricating

Fig. 24 Forming defects in hydroforming of the tubular component with three bulges: **a** splitting on the straight tube blank; **b** splitting on the wrinkled tube blank; **c** undercut on the wrinkled tube blank



the wrinkled tube blank are determined as 250 °C, 4 mm, 5.5 MPa/350 °C, 10 mm, 2 MPa/400 °C, 6 mm, 1.33 MPa. Figure 25(a) shows the hydroforming process for thin-walled

tubular component with three local bulges using a wrinkled tube blank prefabricated with above parameters. It is seen from the figure that the tube blank gradually fills toward the

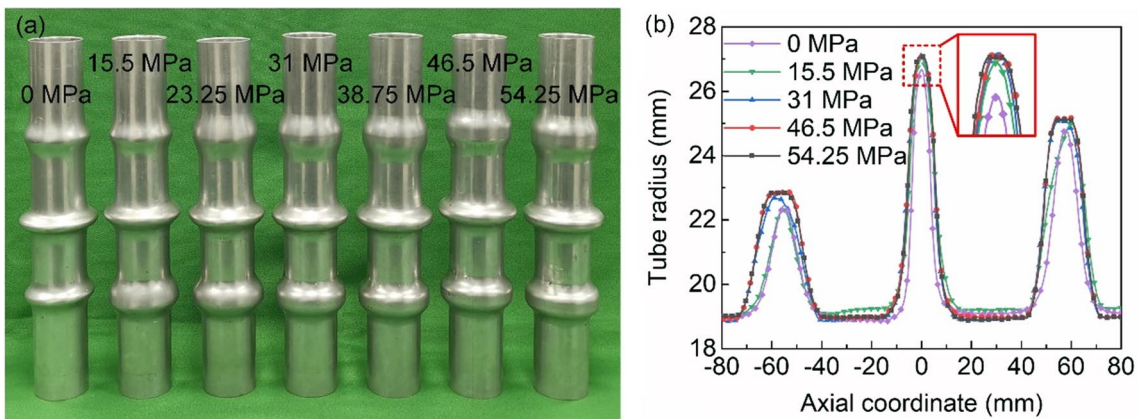


Fig. 25 Hydroforming process for thin-walled tubular component with three local bulges: **a** tube specimens under different internal pressures; **b** evolution of contour shape

bulging zone of the die cavity with the increase of internal pressure. When the internal pressure reaches 46.5 MPa and above, the blank tube has been fully attached to the die cavity at the three bulging zones, and the hydroforming process is completed. This indicates that the wrinkled tube blank obtained under the process parameters of 250 °C, 4 mm, 5.5 MPa/350 °C, 10 mm, 2 MPa /400 °C, 6 mm, 1.33 MPa can be used for the hydroforming of the tubular component with three bulges as shown in Fig. 3.

4.3.3 Tubular component with three bulges and its thickness distribution

Figure 26 shows the hydroformed 5052 aluminum alloy tubular component with three local bulges obtained under the calibration pressure of 54.25 MPa. Figure 27 shows the thickness distribution of the hydroformed 5052 aluminum alloy tubular component with three local bulges. As shown in the figure, thickness thinning occurred in three bulges of the tubular component after hydroforming. The maximum wall thickness thinning ratios at the first, second, and third bulges are 13.41%, 18.62%, and 17.76%, respectively.

5 Conclusion

In this paper, the wrinkling behavior of 5052 aluminum alloy tube blank in a non-uniform temperature field under different conditions and the deformation behavior of wrinkled tube blank in subsequent hydroforming process were deeply investigated. The main conclusions are as follows:

- (1) The proposed hydroforming process for manufacturing tubular component with multiple local bulges was successfully implemented in this investigation based on wrinkled tube blank prefabricating by selective induction heating. It provides a forming method for the fabrication of tubular components with multiple local bulges from hard-to-form materials.

Fig. 26 Hydroformed 5052 aluminum alloy tubular component with three local bulges

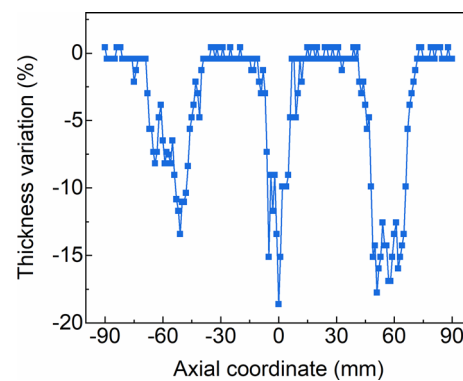
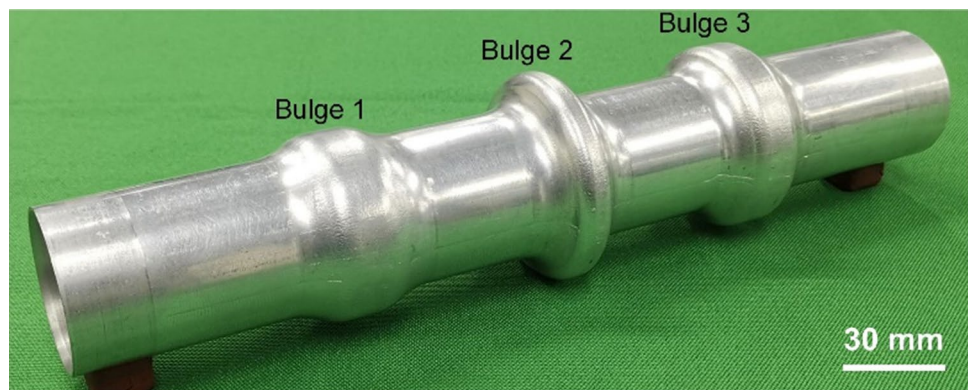


Fig. 27 Thickness distribution of the hydroformed 5052 aluminum alloy tubular component with three local bulges

- (2) The performances of the initial straight tube blank and wrinkled tube blank are evaluated using the hydro-bulging test. Both kinds of tube blanks split along the axial direction. However, the splitting position of the initial tube blank is in the middle of the bulging zone, while that of the wrinkled tube blank is on one side of wrinkle. Moreover, the existence of wrinkles is beneficial to increase the ultimate expansion ratio of the tube blank. Compared with the initial hardened tube blank, the ultimate expansion ratio of the wrinkled tube blank increases from 6.3% to more than 24%.
- (3) Wrinkling behavior of 5052 aluminum alloy tube blank under different conditions and the interaction between wrinkles were investigated by experiments. The process parameters for prefabricating two or three wrinkles, including temperature, spacing between wrinkles, and internal pressure, were determined through a detailed experimental investigation. It is found that the second wrinkle is more likely to be formed when the difference between the maximum force for forming the second wrinkle and the force at the end of forming the first wrinkle is negative. This requires that the temperature at which the next wrinkle is formed is higher than

the temperature at which the previous wrinkles were formed. Under the conditions of appropriate process parameters, multiple wrinkles do not affect each other during wrinkling process. Moreover, the contour shape of two or three axisymmetric wrinkles formed on the tube blank can be accurately fitted using the Gauss function, and their thickness distributions have the same tendency.

- (4) The defects including splitting and undercut that occur in the hydroforming of tubular component with three bulges are analyzed based on the experimental results. After a wrinkled 5052 aluminum alloy tube blank is obtained under the process parameters of 250 °C, 4 mm, 5.5 MPa/350 °C, 10 mm, 2 MPa/400 °C, 6 mm, 1.33 MPa, the final tubular component with three bulges can be hydroformed successfully. Moreover, the thickness distribution of the final hydroformed tubular component with three bulges is discussed. The results of this investigation provide insights for the manufacturing of tubular component with multiple local bulges.

Acknowledgements This investigation is financially supported by the National Natural Science Foundation of China (No. 51805357, U1937205), the Natural Science Foundation of Heilongjiang Province, China (No. LH2022E057), and the China Postdoctoral Science Foundation (No. 2020M670907). The authors wish to express their gratitude to the funding support.

Data availability The raw/processed data required to reproduce the above findings cannot be shared at this time due to technical/time limitations.

Declarations

Conflict of interest We declare that we have no conflict of interest.

Ethical approval This article does not contain any studies with human participants or animals performed by any of the authors.

References

- Reddy PV, Reddy BV, Ramulu PJ. Evolution of hydroforming technologies and its applications—a review. *J Adv Manuf Syst*. 2021;19:737–80. <https://doi.org/10.1142/S0219686720500341>.
- Stojanovic B, Bukvic M, Epler I. Application of aluminum and aluminum alloys in engineering. *Appl Eng Lett*. 2018;3:52–62. <https://doi.org/10.18485/AELETTERS.2018.3.2.2>.
- Kumar D, Phanden RK, Thakur L. A review on environment friendly and lightweight magnesium-based metal matrix composites and alloys. *Mater Today Proc*. 2021;38:359–64. <https://doi.org/10.1016/J.MATPR.2020.07.424>.
- Chu E, Xu Y. Hydroforming of aluminum extrusion tubes for automotive applications Part I: buckling, wrinkling and bursting analyses of aluminum tubes. *Int J Mech Sci*. 2004;46:263–83. <https://doi.org/10.1016/J.IJMECSCI.2004.02.014>.
- Xia ZC. Failure analysis of tubular hydroforming. *J Eng Mater Technol*. 2001;123:423–9. <https://doi.org/10.1115/1.1394966>.
- Strano M. Design and modelling of parts, process and tooling in tube hydroforming. *Hydroforming Adv Manuf*. 2008. <https://doi.org/10.1533/9781845694418.1.121>.
- Yuan S, Wang X, Liu G, Wang ZR. Control and use of wrinkles in tube hydroforming. *J Mater Process Technol*. 2007;182:6–11. <https://doi.org/10.1016/J.JMATPROTEC.2006.06.007>.
- Lang L, Yuan S, Wang X, Wang ZR, Fu Z, Danckert J, Nielsen KB. A study on numerical simulation of hydroforming of aluminum alloy tube. *J Mater Process Technol*. 2004;146:377–88. <https://doi.org/10.1016/J.JMATPROTEC.2003.11.031>.
- Lang L, Li H, Yuan S, Danckert J, Nielsen KB. Investigation into the pre-forming's effect during multi-stages of tube hydroforming of aluminum alloy tube by using useful wrinkles. *J Mater Process Technol*. 2009;209:2553–63. <https://doi.org/10.1016/J.JMATPROTEC.2008.06.027>.
- Tang ZJ, Liu G, Bin He Z, Yuan SJ. Wrinkling behavior of magnesium alloy tube in warm hydroforming. *Trans Nonferrous Met Soc China*. 2010;20:1288–93. [https://doi.org/10.1016/S1003-6326\(09\)60292-2](https://doi.org/10.1016/S1003-6326(09)60292-2).
- Song WJ, Heo SC, Kim J, Kang BS. Investigation on preformed shape design to improve formability in tube hydroforming process using FEM. *J Mater Process Technol*. 2006;177:658–62. <https://doi.org/10.1016/J.JMATPROTEC.2006.04.084>.
- Yuan SJ, Cui XL, Wang XS. Investigation into wrinkling behavior of thin-walled 5A02 aluminum alloy tubes under internal and external pressure. *Int J Mech Sci*. 2015;92:245–58. <https://doi.org/10.1016/J.IJMECSCI.2014.12.017>.
- Kang BH, Lee MY, Shon SM, Moon YH. Forming various shapes of tubular bellows using a single-step hydroforming process. *J Mater Process Technol*. 2007;194:1–6. <https://doi.org/10.1016/J.JMATPROTEC.2007.02.029>.
- Furushima T, Hung NQ, Manabe KI, Sasaki O. Development of semi-dieless metal bellows forming process. *J Mater Process Technol*. 2013;213:1406–11. <https://doi.org/10.1016/J.JMATPROTEC.2013.03.002>.
- Zhang Z, Furushima T, Manabe K, Tada K, Sasaki O. Development of dieless metal bellows forming process with local heating technique. *Proceed Inst Mech Eng Part B J Eng Manuf*. 2014;229:664–9. <https://doi.org/10.1177/0954405413519610>.
- Sedighi M, Shamsi M. A new approach in producing metal bellows by local arc heating: a parametric study. *Int J Adv Manuf Technol*. 2017;939:3211–9. <https://doi.org/10.1007/S00170-017-0768-1>.
- Cui XL, Lin P, Chi CZ. Beneficial wrinkle prefabrication method for improving high-pressure forming limit in tube, n.d. <https://www.wanfangdata.com.cn/patent/ChJQYXRlbnROZXdtMjAyMjAzMjMSE0NOMjAxOTEwMjE2MTg2Ljdfc3EaCGh6Z2x0M3NI> (accessed November 17, 2020).
- Cui XL, Guo J, Wen SY, Wu XM, Lin P. Plastic wrinkling of thin-walled tubes under axial compression in non-uniform temperature field. *Proc Inst Mech Eng Part C J Mech Eng Sci*. 2022;237:406–19. <https://doi.org/10.1177/09544062221121987>.
- Benham PP, Crawford RJ, Armstrong CG. *Mechanics of engineering materials*, 2nd ed. Harlow, Essex: Longman; 1996.

Publisher's Note Springer Nature remains neutral with regard to jurisdictional claims in published maps and institutional affiliations.

Springer Nature or its licensor (e.g. a society or other partner) holds exclusive rights to this article under a publishing agreement with the author(s) or other rightsholder(s); author self-archiving of the accepted manuscript version of this article is solely governed by the terms of such publishing agreement and applicable law.